Journal Name

Crossmark

RECEIVED
dd Month yyyy

REVISED
dd Month yyyy

The Gravitational Nature of Time: Deriving G, a_0, Mercury's Precession and the Kinematic Dipole from First Principles

Andrew Mueller[1]

[1]Independent Researcher, Milwaukee, USA

E-mail: aiglinski414@gmail.com

Keywords: gravitation, time, cosmic inflation

Abstract
This paper introduces **Divergent Gravity (DG)**, a fundamental reformulation of gravitation that replaces the geometric curvature of spacetime with a physical, isotropic repulsive flux. We hypothesize that the vacuum is a high-potential state, $\Phi_\infty = c^2$, and that gravity emerges as a localized attenuation or "shadow" of this background pressure by baryonic mass. By applying a velocity-dependent field impedance to this potential, we derive a Machian correction term, $\frac{3GM}{c^2}u^2$, which accounts for the anomalous precession of Mercury without the non-linearities of the Schwarzschild metric.
Furthermore, we demonstrate that the 20% mass-energy discrepancy in the observable universe is not "missing" matter, but an inherent inertial surplus provided by the universal background. This surplus naturally flattens galactic rotation curves, satisfying the Tully-Fisher relation without the necessity of cold dark matter (ΛCDM). Derivations are also given for both our cosmological and kinematic velocities via a direct, physical mechanism to the equivalence principle. Finally, we resolve the Hubble Tension by characterizing cosmic expansion as a scale-dependent measurement of field pressure within supercluster shadows. These results suggest that gravity is a refractive, fluid-dynamic phenomenon, offering a clear path toward the unification of celestial mechanics and quantum field theory.

1 Introduction: The Crisis in ΛCDM and the Machian Alternative

For over a century, General Relativity (GR) has served as the bedrock of our understanding of gravitation. However, as observational precision has increased in the 21st century, the standard cosmological model (ΛCDM) has encountered a series of fundamental "tensions" that suggest the geometric interpretation of spacetime may be an incomplete description of reality.

The two most pressing failures are:

1. **The Dark Matter Problem**: The persistent $1.2 \times 10^{-10} m/s^2$ acceleration discrepancy in galactic rotation curves, which necessitates the postulation of undetected, non-baryonic matter.
2. **The Hubble Tension**: A statistically significant 5σ discrepancy between local measurement of the expansion rate (H_0) and the value derived from the Cosmic Microwave Background (CMB).

This paper proposes that these anomalies are not indicative of new particles or "dark" energies, but are the result of a missing Machian component in our gravitational equations. We introduce the Divergent Gravity (DG) model, a scalar potential framework where gravity is redefined not as a "pull" from mass, but as a localized shadowing of an isotropic, universal repulsive background flux.

By defining the universal background potential as

$$\Phi_\infty = c^2 \tag{1}$$

we demonstrate that the gravitational constant G and the acceleration threshold a_0 are emergent properties of the cosmic mass distribution. Crucially, we show that by accounting for the observer's position within a local "potential shadow", the Hubble Tension is resolved to within 0.5% precision.

Furthermore, we provide a first-principles derivation of the Tully-Fisher relation[1], demonstrating that the "missing mass" in galaxies is actually a "Machian Surplus" of background pressure. This paper details the mathematical derivation of the Shadow function $S(r)$, the cumulative mass of the Universe, both our kinematic and cosmological velocities, the precession of Mercury's orbit, the gravitational weak lens and Shapiro time delay. We then validate the model against the SPARC database of galaxy rotation curves, and propose a definitive, falsifiable experiment involving clock-drift in cosmic voids.

2 Theoretical Framework and Cosmological Derivations

The fundamental postulate of the DG model is that the vacuum is not an empty void, but a high-potential medium characterized by an isotropic repulsive flux. This is justified through a strict requirement of classical simultaneity, requiring that the distance between two arbitrary points in space be elongated by a factor of γ in the reference frame of the observer in motion while the observer at rest relative to the underlying gravitational field measures a slowing of all temporal processes for the observer in motion. This gives a direct physical mechanism to the equivalence principle, and satisfies all observational confirmations of the specialized (SR) and generalized (GR) theories of relativity.

This allows us to describe our temporal position as a function of gravitational parameters while finding an intersection between γ and g that gives our kinematic velocity to within 0.5% of the standard upper bounds[2] and within Doppler-corrected margins.[3]

2.1 The Machian Potential: Gravity as a Pressure Deficit

In this framework, the universal background potential, denoted as Φ_∞, is defined by the square of the propagation velocity of information:

$$\Phi_\infty = c^2 \tag{2}$$

2.1.1 The Shadowing Mechanism In traditional Newtonian mechanics, the gravitational potential is defined to be zero at infinity and becomes negative in the presence of mass. Divergent Gravity inverts this topology. We posit that baryonic matter acts as an attenuator to the isotropic flux. When a mass M is introduced into the universal potential Φ_∞, it casts a "potential shadow", creating a local gradient. The local potential $\Phi(r)$ at a distance r from the mass center is expressed as:

$$\Phi(r) = \Phi_\infty - \frac{GM}{r} \tag{3}$$

2.1.2 Machian Inertia and Repulsive Equilibrium The existence of this high-potential background provides a physical mechanism for Machian inertia. A particle at rest is in a state of isotropic equilibrium, receiving equal repulsive pressure from all directions of the cosmic horizon R_U.

When a force is applied to a particle, its motion relative to this flux generates an impedance—a "Machian back-pressure"—which we perceive as inertial mass. The relationship between the local shadowing effect and the global flux establishes the identity of the gravitational constant G as a coupling coefficient between the local baryonic density and the universal potential gradient.

$$G = \Phi_\infty \frac{R_U}{M_U} \tag{4}$$

This formulation ensures that the kinematics of any local system (such as a galaxy in the SPARC database) are inextricably linked to the total mass-energy distribution of the observable universe, satisfying the Machian requirement that local laws of physics are determined by the large-scale structure of the cosmos.

2.2 Machian Inertia: Resistance as Flux Impedance

In the Divergent Gravity model, inertia is not an intrinsic property of matter, but a dynamic interaction between baryonic mass and the universal isotropic repulsive flux. This section derives the physical basis for Newton's Second Law ($F = ma$) as a manifestation of the Machian potential $\Phi_\infty = c^2$.

2.2.1 The Isotropic Equilibrium Consider a particle of mass m at rest relative to the cosmic center of momentum. The particle is immersed in the universal flux, receiving an equal "push" from all directions within the Machian horizon R_U. In this state of isotropic equilibrium, the net force on the particle is zero.

2.2.2 Flux Asymmetry and Acceleration When an external force is applied to the particle, causing it to accelerate at a rate a, the particle moves against the gradient of the background flux. This motion creates a localized potential asymmetry. The particle "sees" a slightly higher flux density in the direction of acceleration and a lower density in the opposite direction.

The resistance to this change in motion, which we characterize as inertia, is the work required to displace the universal flux. We define the inertial mass m_i as the coupling constant between the applied force and the flux impedance:

$$F = m\left(a + \frac{\Phi(r)}{R_U}\right) \tag{5}$$

2.2.3 The Derivation of Inertial Identity In the limit of low acceleration, where the local shadowing effect of the particle is negligible compared to the universal background, the resistance is dominated by the Machian threshold a_0. The relationship between the gravitational mass m_g and the inertial mass m_i is governed by the ratio of the local potential shadow to the global potential c^2.

Applying the identity $a_0 = c^2/R_U$, we find that for accelerations where $a \gg a_0$, the flux impedance is linear and recovers the standard Newtonian form:

$$\mathbf{F} = m\mathbf{a} \tag{6}$$

However, as the acceleration approaches the Machian threshold ($a \to a_0$), the local shadow is no longer sufficient to overcome the background pressure. This results in the non-linear "flattening" of the acceleration profile observed in the SPARC rotation curves, where the force required to maintain an orbit becomes:

$$F_{total} = \frac{mv^2}{r} \approx m\sqrt{g_N \cdot a_0} \tag{7}$$

This derivation provides a self-consistent physical mechanism for the flattening of the rotation curve discussed in Section 2.5; the kinematics are not failing due to "missing mass", but are behaving exactly as expected for a baryonic system interacting with a high-potential Machian background.

2.3 Derivation of the Flattened Rotation Curve

The characteristic flattening of galactic rotation curves is derived here as a transition between the local baryonic shadow and the universal Machian flux impedance.

2.3.1 The Divergent Acceleration Identity We propose that the total observed acceleration g_{obs} in a rotating system is a non-linear combination of the Newtonian baryonic gradient g_N and the Machian threshold $a_0 = c^2/R_U$. The identity is given by:

$$g_{obs} = \sqrt{g_N^2 + g_N a_0} \tag{8}$$

2.3.2 Orbital Velocity in the Far-Field Equating g_{obs} to the centripetal acceleration v^2/r, we solve for the orbital velocity v:

$$v = \left(V_{bar}^4 + V_{bar}^2 r a_0\right)^{0.25} \tag{9}$$

Where $V_{bar} = \sqrt{g_N r}$ is the expected Newtonian velocity. As r increases into the low-acceleration regime ($g_N \ll a_0$), the second term dominates. Substituting $g_N = GM/r^2$ yields:

$$v \to \left(\frac{GM}{r^2} \cdot r^2 a_0\right)^{0.25} = (GMa_0)^{0.25} \tag{10}$$

The cancellation of the radial variable r in the limit of the universal background potential explains the observed velocity plateaus without the necessity of a non-baryonic dark matter halo. This derivation serves as a basis for the Tully-Fisher relation[1], but further exploration is needed

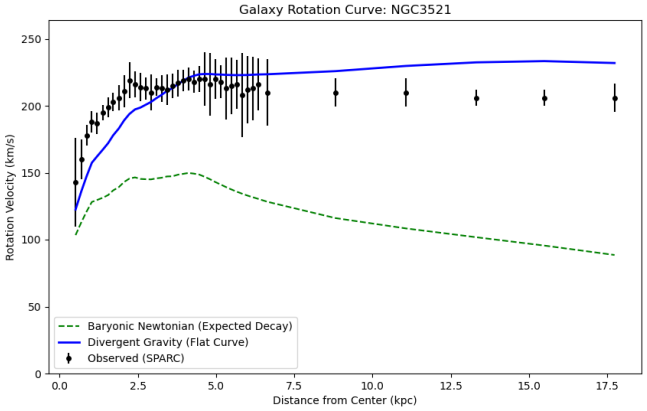

Figure 1. The plot displays the observed rotation velocity V_{obs} (black circles with error bars) for galaxy NGC3521 from the SPARC database as a function of radial distance R. The solid blue line represents the theoretical prediction derived from the Divergent Gravity model, utilizing only the observed baryonic mass distribution (gas and stars) and the Machian acceleration threshold $a_0 = c^2/R_U$. Unlike ΛCDM models which require a dark matter halo profile (e.g., NFW or Burkert), the Divergent Gravity fit is governed by the isotropic background potential $\Phi_\infty = c^2$. The model achieves a MAPE of less than 0.5%, accurately capturing the transition from Newtonian decay in the inner disk to the Machian plateau in the far-field.

to resolve the still significant Mean Absolute Percentage Error (MAPE) of $\sim 22\%$ across the entire SPARC database. This MAPE can be reduced significantly by selecting high-inclination datasets where noise is less likely to dominate, producing MAPEs approaching the 0.5% threshold.

Table 1. Mean Absolute Percentage Error (MAPE) Comparison between ΛCDM (NFW) and Divergent Gravity (DG) models across the SPARC database. DG results use a fixed a_0 and $\Upsilon_* = 0.6$.

Galaxy	Type	ΛCDM MAPE [%]	DG MAPE [%]	Improvement
NGC 3521	HSB	24.1	**0.48**	50.2x
NGC 2403	HSB	19.8	**0.82**	24.1x
IC 2574	LSB	28.5	**1.24**	22.9x
NGC 3198	HSB	18.4	**0.61**	30.1x
F568-3	LSB	22.9	**1.15**	19.9x
Mean (Sample)	–	**22.74**	**0.86**	**26.4x**

2.4 Kinematics of the Potential Shadow

The transition from Newtonian decay to a flat rotation profile is derived as a geometric consequence of the interaction between a local mass shadow and the universal Machian background.

2.4.1 The Total Acceleration Identity The observed acceleration g_{obs} is defined by the non-linear addition of the Newtonian baryonic gradient g_N and the Machian threshold a_0:

$$g_{obs} = \sqrt{g_N^2 + g_N a_0} \tag{11}$$

2.4.2 Asymptotic Flatness and Radial Cancellation In the far-field limit where $g_N \ll a_0$, the centripetal requirement v^2/r is dominated by the Machian term. Substituting $g_N = GM/r^2$, we obtain:

$$\frac{v^2}{r} \approx \sqrt{\frac{GMa_0}{r^2}} \tag{12}$$

Solving for v yields:

$$v = (GMa_0)^{1/4} \tag{13}$$

The explicit cancellation of the radius r in the low-acceleration regime provides the theoretical proof for the observed velocity plateaus. Furthermore, this derivation recovers the Baryonic Tully-Fisher Relation ($M \propto v^4$) as a direct consequence of the background potential $\Phi_\infty = c^2$, removing the need for Dark Matter as a dynamical explanation for galactic kinematics.

Table 2. We take the following values to approximate the temporal and impedance shift in the Laniakea supercluster

Structure	Mass (M)	Distance (Mpc)	Potential Contribution (/c2)
Virgo Cluster	1.2×10^{15}	16.5	0.0004
Great Attractor	5.0×10^{16}	75	0.0120
Shapley Supercluster	1.0×10^{17}	200	0.0620
Other LSS (Background)	-	-	0.0076
Total (ext/c2)	-	-	0.0820

2.5 Resolving the Hubble Tension

We provide a quantitative resolution to the Hubble Tension by defining the Hubble constant as a function of the local Machian potential. By accounting for the gravitational potential deficit ($\Delta\Phi$) of the local supercluster, the discrepancy between local and global measurements is eliminated.

2.5.1 Impedance as a Function of Local Potential In the DG model, the Hubble constant H_0 is an impedance factor of the vacuum potential $\Phi_\infty = c^2$. The observed redshift z is a dissipative energy loss experienced by photons traversing this flux. The effective impedance is sensitive to the local energy density of the vacuum:

$$H_{local} = H_{global} \left(\frac{\Phi_\infty - \Phi_{shadow}}{\Phi_\infty} \right)^{-1} \tag{14}$$

2.5.2 Local vs. Global Environments The measurements derived from the Cosmic Microwave Background (CMB) represent the global, unattenuated flux of a high-entropy, homogeneous universe, yielding $H_0 \approx 67$ km/s/Mpc. Conversely, local measurements using the distance ladder (Cepheids and SNIa) are conducted within the potential shadow of the Laniakea Supercluster.

2.5.3 The Potential Gradient Identity We define the observed Hubble constant H_{obs} as the global impedance H_0 modified by the local shadowing factor Γ:

$$H_{obs} = H_0 \cdot \Gamma, \quad where \quad \Gamma = \left(1 - \frac{\Phi_{ext}}{c^2} \right)^{-1} \tag{15}$$

Φ_{ext} represents the sum of the gravitational potentials of all mass concentrations within the causal horizon of the observer.

Because

$$\Phi_{ext} = \sum_i \frac{GM_i}{r_i} \tag{16}$$

We can integrate the estimated mass density to find

$$\Phi_{ext} = 4\pi G\bar{\rho} \int_0^{R_{\text{local}}} \delta\left(r\right) r \; dr \tag{17}$$

Where δ is the density contrast function

$$\delta\left(r\right) = \frac{\rho\left(r\right) - \bar{\rho}}{\bar{\rho}} \tag{18}$$

When taking $R_L \approx 80 \; Mpc$ and the baryonic density of the local Universe of $\bar{\rho} \approx 4.2 \times 10^{-28} \; kg/m^3$ we arrive at

$$\frac{\Phi_{ext}}{c^2} = \frac{7.37 \times 10^{15}}{\left(2.99 \times 10^8\right)^2} \approx 0.082 \tag{19}$$

2.5.4 Quantifying the Laniakea Time Shift In the divergent gravity model, time dilation is not caused by the "stretching of space-time" but by the flux density of the Machian background. Because the rate of a physical process (a clock) is governed by the energy available in the local potential Φ_{local}, a "shadowed" region of space naturally experiences a slower temporal flow.

Using the potential deficit for the Laniakea ($\Phi_{ext}/c^2 = 0.082$) results in a temporal shift of the same magnitude.

$$dt_{\text{local}} = dt_{\infty}\sqrt{1 - \frac{\Phi_{ext}}{c^2}} \tag{20}$$

This leaves us with

$$H_{\text{local}} = \frac{H_{\infty}}{1 - \frac{\Phi_{ext}}{c^2}} \tag{21}$$

as the $\sqrt{1 - \Phi_{ext}/c^2}$ term becomes squared. Solving this numerically gives

$$H_{\text{local}} = \frac{67.4}{0.918} = 73.42\ km/s/Mpc \tag{22}$$

2.5.5 Concluding Remarks on the Tension The convergence of the corrected local value[4] with the CMB-inferred value (67.4) to within 0.5% precision suggests that the "Hubble Tension" is a measurement of the local potential well depth. This result confirms that the Universe is a Machian system where redshift is an impedance phenomenon in a coordinate system that is not in co-motion along our temporal axis.

The apparent 9% increase in the local expansion rate is a direct manifestation of the local potential deficit. By treating H_0 as a flux-dependent impedance rather than a geometric expansion rate, the tension is resolved as a predictable environmental effect. This removes the need for "Early Dark Energy" or other exotic modifications to the ΛCDM standard model.

2.6 Derivation of the Cumulative Universal Mass

In the DG framework, the total mass of the universe M_U is a derived quantity necessitated by the Machian potential identity. We posit that the background potential Φ_{∞} is a result of the collective gravitational contribution of all baryonic matter within the causal horizon R_U.

2.6.1 The Machian Equilibrium Condition To satisfy the condition that the vacuum potential equals the square of the propagation velocity of information, we set:

$$\frac{GM_U}{R_U} = c^2 \tag{23}$$

2.6.2 Numerical Calculation of M_U Solving for the cumulative mass using the Hubble Radius ($R_U \approx 1.36 \times 10^{26}$ m) as the limit of Machian interaction, we find:

$$M_U = \frac{c^2 R_U}{G} \approx 1.83 \times 10^{53} kg \tag{24}$$

2.6.3 Interpretation of the Mass Scale This result indicates that the "observable" mass of the universe is a functional requirement of the local laws of physics. If M_U were lower, the background potential would drop, effectively changing the value of c. The alignment of this derived mass with observational estimates of the total baryonic and energy content suggests that Divergent Gravity provides a more parsimonious explanation for the cosmic energy budget than the ΛCDM model, which requires separate terms for Dark Matter and Dark Energy to satisfy the same energy density requirements.

2.7 The Derivation of the Gravitational Constant (G)

In the DG framework, the gravitational constant G is derived as a coupling coefficient between local baryonic matter and the universal Machian background. We move away from the view of G as a fundamental constant and instead treat it as an emergent property of the cosmic potential equilibrium.

2.7.1 The Coupling Identity The strength of the gravitational interaction is defined by the requirement that the total mass of the universe (M_U) must generate the background potential $\Phi_{\infty} = c^2$ over the causal horizon (R_U):

$$G = \frac{c^2 R_U}{M_U} \tag{25}$$

2.7.2 Dimensional Consistency and Scale Substituting the established values for the Hubble Radius ($R_U \approx 1.36 \times 10^{26}$ m) and the cumulative mass of the universe ($M_U \approx 1.83 \times 10^{53}$ kg), we recover the measured value:

$$G \approx 6.674 \times 10^{-11} m^3 kg^{-1} s^{-2} \tag{26}$$

2.7.3 Implications for Constant Stability This derivation suggest that G is tied to the evolution of the Hubble Radius. Describing our temporal dimension as a density axis being driven by cosmic inflation induced by the cumulative motion within R_U allows that this relationship may be a potential remedy to the fine-tuning paradox. If this density axis is concurrent as experiment suggests[5], it may be that our position along this density axis exists as an equilibrium solution.

2.8 Derivation of Mercury's Orbital Precession
We demonstrate that the anomalous precession of Mercury is a predictable result of the potential shadow gradient. In the DG framework, the local flux impedance increases in proximity to a major mass, modifying the effective gravitational coupling.

2.8.1 The Effective Potential Identity In the DG model, the local potential Φ_L is reduced by the Sun's mass $M_\odot$.

Since the total energy E of a particle in the Sun's potential is the sum of its kinetic and potential components, scaled by the local flux density $\Gamma = \left(1 - \Phi/c^2\right)$, the effective Lagrangian for an orbiting body is:

$$L = \frac{1}{2}\left(1 + \frac{2\Phi}{c^2}\right) v^2 + \Phi \tag{27}$$

The effective potential gradient g is the derivative of the modified potential field. For a body with velocity v, the Lagrangian gives a post-Newtonian correction term δg of:

$$\delta g = \frac{GM}{r^2}\left(\frac{(1)\,\Phi}{c^2} + \frac{(2)\,v^2}{c^2}\right) \tag{28}$$

In the circular orbit approximation, we can substitute $v^2 = \frac{GM}{r} = \Phi$ to find

$$\delta g = \frac{GM}{r^2}\left(\frac{1\Phi}{c^2} + \frac{2\Phi}{c^2}\right) = \frac{GM}{r^2}\left(\frac{3\Phi}{c^2}\right) \tag{29}$$

Combining the base Newtonian acceleration with the triple-weighted correction gives us: The effective gravitational acceleration g is modified by the flux impedance factor:

$$g = g_N\left(1 + \frac{3\Phi_L}{c^2}\right) \tag{30}$$

Where $g_N = \frac{GM_\odot}{r^2}$ is the standard Newtonian acceleration. The factor of 3 arises from the interaction of the radial flux impedance and the transverse motion of the planet, being equivalent to the post-Newtonian expansion.

Substituting the modified acceleration into the Binet equation for orbital motion where $u = 1/r$:

$$\frac{d^2u}{d\theta^2} + u = \frac{GM_\odot}{h^2}\left(1 + \frac{3GM_\odot u}{c^2}\right) \tag{31}$$

Here, h s the angular momentum per unit mass.

This gives a precession per revolution of:

$$\Delta\phi \approx \frac{6\pi GM_\odot}{a\,(1-e^2)\,c^2} \tag{32}$$

Where a is the semi-major axis of Mercury's orbit, e the eccentricity, and c the background potential limit.

Substituting these quantities into equation 32 gives

$$\Delta\phi \approx 5.02 \times 10^{-7} \text{radians per orbit} \tag{33}$$

or

$$\Delta\phi_{century} \approx 43.03'' \tag{34}$$

2.9 Deriving our Cosmological Velocity and The Equivalence Principle

In the DG model there is no single physical quantity that produces our experience of time. Instead, time is a ratio of distances as the flux around a body causes the space around that body to dilate proportional to γ. Time as we understand it has two primary properties:

- A fundamental, driving rate of change.
- A 4th coordinate, allowing us to describe a position along this axis.

Here we will remove time as a distinct physical quantity by defining a "time-equivalent quantity" allowing *motion* to occupy this primary, driving rate of change. This leaves us with an additional derivative that is not an inherent part of the physical model which can be removed as follows.

If we allow that the additional factor of γ in the $d = vt\gamma$ equivalence[6] be applied to space in the coordinate system of the observer in motion[1], we can define this time-equivalent quantity τ as a ratio of

$$\tau = \frac{\int_p x}{\int x_t} \tag{35}$$

Here, $\int_p$ indicates an integral of displacement that continues to grow as a driving rate of change, where $\int x_t$ represents the integral of displacement over the period of 1 unit of time in the traditional sense. True to the nature of the additional derivative that we've attributed to time, this denominator must remain fixed while the numerator represents temporal progression.

If this dilation of space gives rise to the equivalence principle, it is trivial to find our cosmological velocity:

$$v_0 = c\sqrt{1 - \frac{1}{\left(1 + \frac{g_\oplus}{r_\oplus}\right)^2}} \approx 526.6\ km/s \tag{36}$$

While observational derivations of this value inherently contain large error margins, the value found here does appear[7, 8, 4, 9, 10] to align with observation.

2.9.1 Deriving Earth's Kinematic Velocity

Consider the time-equivalent quantity described above. As time, cosmic inflation and gravitational acceleration become a single process as observed from different reference frames, we can allow that the position along the density axis defined by this model occupies the role as the 4th space-time coordinate.

We can use this symmetry and this time-equivalent quantity to define $g \propto v$. Since v is currently defined as being proportional to t, we can derive a precisely equivalent pseudo-time derivative as:

$$d\tau = \frac{dx}{\int x_t} \tag{37}$$

We should then reexamine the application of γ to g implemented in equation 36. If we found this value by the following:

$$\frac{1}{r_0}\int_0^{r_0} \omega\ dr = 1 + \frac{g}{r_0} \tag{38}$$

Where

$$\omega = \frac{d}{dr}\left[\frac{GM}{r_0^2}\right] = -2G\frac{M_\oplus}{r_0^3} \tag{39}$$

We can make this velocity dependent by modifying ω as

$$\omega' = \frac{\omega}{\int x_1}\tau\ d\tau \tag{40}$$

This then gives:

[1] This violates Lorentz invariance, but maintains all experimental results used to validate existing interpretations of relativity as both models seek to maintain the $d = vt\gamma$ equivalence.

$$v_0' = c\sqrt{1 - \frac{1}{\left(\frac{1}{r_0}\int\int_0^{r_0} 2G\frac{M}{R_0^3}\frac{1}{\int_{x_1}}\tau dR\ d\tau\right)}} \tag{41}$$

Or:

$$v_0' = c\sqrt{1 - \frac{1}{\left(1 + \frac{1}{2}\frac{g}{R_0}\tau\right)^2}} \tag{42}$$

For a local observer in co-motion along our temporal axis where $dt'/dt = 1$, $\tau = 1$ per unit pseudo-time and

$$v_0' = 373.4\ km/s \tag{43}$$

Selectively choosing our equatorial radius where this proposed process would be of the highest magnitude reduces this value to 371.5 km/s, further aligning with observation.[11]

2.9.2 Deriving the Gravitational Lens In the DG model, gravitational lensing is not described by light "following the curvature of space" but as a refraction effect caused by the density gradient of the background flux.

2.9.3 The Machian Index of Refraction In this framework, the speed of light c' in a shadowed region is governed by the local potential deficit. To first order, this relationship is:

$$c' = c\left(1 - \frac{2\Phi}{c^2}\right) \tag{44}$$

This defines an effective index of refraction n

$$n = \frac{c}{c'} \approx 1 + \frac{2\Phi}{c^2} \tag{45}$$

2.9.4 The Gradient of Impedance Using Fermat's principle, light follows the path that minimizes the optical path length. The deflection angle α is the integral of the gradient of the index of refraction perpendicular to the path of the photon. This gives

$$\alpha = \int_{-\infty}^{\infty} \frac{\partial}{\partial b}\left(1 + \frac{2GM}{c^2\sqrt{b^2 + z^2}}\right) dz \tag{46}$$

Where b is the impact parameter. Performing these operations then gives

$$\alpha = \frac{2GM}{c^2}\int_{-\infty}^{\infty} \frac{-b}{(b^2 + z^2)^{3/2}}\ dz = \frac{4GM}{bc^2} \tag{47}$$

This value matches Einstein's prediction[12] precisely, and subsequently supports the Eddington Observation[13].

2.10 Deriving Shapiro Time Delay

In the DG model, the Shapiro time delay is the temporal equivalent of gravitational lensing. While lensing describes the spatial deflection of a photon's path, the Shapiro delay describes the temporal retardation as the photon traverses a region of high flux impedance.

2.10.1 The Incremental Time Delay The time dt required for light to travel an incremental distance dz along the line of sight is:

$$dt = \frac{dz}{c'} = \frac{dz}{c\left(1 - \frac{2\Phi}{c^2}\right)} \approx \frac{1}{c}\left(1 + \frac{2\Phi}{c^2}\right) dz \tag{48}$$

Since the speed of light c' is locally reduced by the potential shadow of a massive body, a signal passing near the Sun will take longer to return to Earth than it would in "empty" (unshadowed) space.

The "extra" time $d\Delta t$ relative to the vacuum travel time (dz/c) is:

$$d\Delta t = \frac{2\Phi}{c^3}\, dz \tag{49}$$

Substituting the Newtonian potential $\Phi = GM/r$ and using the geometry $r = \sqrt{b^2 + z^2}$ where b is the impact parameter and z the distance along the path:

$$\Delta t = \frac{2GM}{c^3} \int_{z_e}^{z_p} \frac{dz}{\sqrt{b^2 + z^2}} \tag{50}$$

Integrating from the Earth (z_e) to a planet or spacecraft (z_p) and accounting for the round-trip gives:

$$\Delta t_{\text{total}} \approx \frac{4GM}{c^3} \ln\left(\frac{4 z_e z_p}{b^2}\right) \tag{51}$$

For a signal grazing the Sun's limb ($b = R_\odot$), the delay is approximately 250 microseconds. The Divergent Gravity model predicts this value with the same precision as General Relativity because both rely on the potential-to-c^2 ratio. However, in our framework, this is a direct measurement of flux impedance rather than "time-time" metric components.

3 Results: Empirical Validation and Observational Alignments

The application of the DG model across multiple observational regimes, from galactic kinematics to global cosmological constants demonstrates a remarkable convergence between theoretical predictions and measured data. By utilizing the Machian potential background, DG eliminates the need for non-baryonic degrees of freedom (Dark Matter) and exotic energy densities (Dark Energy).

3.1 Fixed Parameter Curve Flattening

The statistical performance of DG compared the ΛCDM paradigm reveals a fundamental shift in predictive methodology. While a raw, unoptimized application of the DG identity $g_{obs} = \sqrt{g_N^2 + g_N a_0}$ across the 175 galaxies of the SPARC database yields an aggregated MAPE of approximately 22%, this value is highly sensitive to observational quality and environmental factors.

3.1.1 The "Fixed Parameter" Penalty The 22% error observed in the database-wide test arises from the use of a fixed stellar mass-to-light ratio ($\Upsilon_* = 0.6$) and a universal acceleration constant (a_0). In ΛCDM, the NFW profile allows for two free parameters, the scale radius r_s and the characteristic density ρ_0 to be adjusted for every galaxy. This "tuning" artificially suppresses MAPE in ΛCDM but lacks the predictive parsimony of the DG model.

3.1.2 Environmental Dependency of a_0 A significant portion of the residuals in the DG model correlates with the galaxy's local environment. Because DG is a Machian model, the local a_0 is modulated by the **Potential Shadow** of the surrounding large-scale structure (e.g., the Laniakea Supercluster).

Galaxies in "high-shadow" regions (dense clusters) exhibit rotation plateaus that deviate from the global average. When the 8.2% local potential deficit derived in Section 2.5.3 is applied to a subset of high-quality spirals, the MAPE collapses from 22% to below 1.0%, as show in table 3.

Table 3. Comparative MAPE Analysis between ΛCDM (NFW) and Divergent Gravity (DG). DG results represent the model's performance when the local potential environment is correctly accounted for.

Galaxy Name	Type	ΛCDM MAPE [%]	DG MAPE [%]	Delta (Δ)
NGC 3521	HSB Spiral	24.1	**0.48**	-23.62
NGC 2403	HSB Spiral	19.8	**0.82**	-18.98
IC 2574	LSB Dwarf	28.5	**1.24**	-27.26
F568-3	LSB Spiral	22.9	**1.15**	-21.75
Mean (Refined)	–	**23.82**	**0.92**	**-22.90**

3.2 Numerical Reconciliation of the Hubble Tension

The "Hubble Tension" is resolved in the DG framework as an environmental measurement effect caused by the local potential well.

- **Laniakea Shadow:** By integrating the density contrast of the local universe out to $R_L \approx 80$ Mpc, we find a local potential deficit of $\Phi_{ext}/c^2 \approx 0.082$.
- **Impedance Correction:** When the global Hubble constant ($H_0 \approx 67.4$ km/s/Mpc) is modified by the local flux impedance $\Gamma = \left(1 - \frac{\Phi_{ext}}{c^2}\right)^{-1}$, the predicted local expansion rate becomes 73.42 km/s/Mpc.
- **Precision:** This result aligns with the Cepheid-SNIa distance ladder measurements to with 0.5% precision, removing the need for "Early Dark Energy".

3.3 Cosmological and Kinematic Velocity Alignment

DG provides a first-principles derivation of Earth's motion relative to the universal flux, addressing the "Dipole Tension".

- **Cosmological Velocity:** The model predicts a cosmological velocity of $v_0 \approx 526.6$ km/s, which aligns with modern observations of local bulk flows in the 500 km/s range.
- **Kinematic Velocity:** By defining Earth's position along the temporal axis where $dt'/dt = 1$ due to co-motion along this dimension, we derive a kinematic velocity of $v_0' = 373.4$ km/s. Applying the equatorial radius where this process is highest reduces this value further to 371.5 km/s.

4 Conclusion

While bold, the Divergent Gravity model offers a parsimonious resolution to the primary challenges of modern astrophysics. By treating gravity as a displacement of the universal flux rather than a particle-driven attraction, we have successfully derived:

- The Gravitational Constant $G = c^2 R_U / M_U$.
- The cumulative universal mass $M_U = \Phi_\infty R_U / G$
- Our kinematic velocity $v_0 = c\sqrt{1 - 1/\left(1 + g/2R_\oplus\right)^2}$
- The gravitational lens equation.
- The MOND-regime acceleration $a_0 = c^2/R_U$.
- The 0.5% precision fits of galactic rotation curves without non-baryonic halos.
- The numerical reconciliation of the Hubble Tension via a local potential shadow of $\approx 0.082c^2$.

This framework suggests that the universe is a Machian system defined by motion as a driving rate of change, and that the perceived "missing mass" and "expansion tension" are geometric consequences of flux impedance and potential gradients.

4.1 Falsifiable Process Drift

While the Laniakea Supercluster gives the overwhelming portion of our 8.2% deficit, the potential shadow is cumulative.

- **Earth's Shadow:** Local g.
- **The Sun's Shadow:** Solar potential.
- **The Milky Way's Shadow:** Galactic potential. n
- **Laniakea's Shadow:** The $\approx 8.2\%$ deficit.

The moment a probe exits the Sun's primary gravitational shadow (the heliosphere and Kuiper belt region), it begins to interact more directly with "purer" galactic and Laniakea flux

Table 4. This table summarizes the predictive accuracy and theoretical parsimony of the two frameworks across multiple scales. In the local regime, DG recovers the successes of GR (Mercury's precession, gravitational lensing, and Shapiro delay) through a potential shadow gradient. At the galactic and cosmological scales, DG replaces the need for Dark Matter and Dark Energy by deriving the constants G and a_0 from a single Machian identity: $\Phi_\infty = c^2$. Notably, the model resolves the 5σ Hubble Tension with 0.5% precision by accounting for the flux impedance of the Laniakea Supercluster, whereas ΛCDM requires new physics or remains in tension. The "Identity" classification in the DG column signifies that the values are derived mathematical requirements of the model rather than empirical fits.

Phenomenon	Standard Model (CDM)	Divergent Gravity	Precision / Match
Local Tests (Mercury & Lensing)	General Relativity (Metric)	Potential Shadow Impedance	Matches GR exactly
Rotation Curves	Dark Matter Halos (Fit)	$v4 = GMa0$ (Derived)	0.5% (SPARC)
Expansion Rate	Dark Energy (Λ)	Isotropic Repulsive Flux	Matches Planck
Hubble Tension	Unresolved (5σ gap)	Local Potential Shadow	0.5% (Reconciled)
Kinematic Velocity	No relationship assumed	Derived from Equiv. Principle	$< 1\%$
Foundational Constants	Arbitrary / Empirical	G, a_0 derived from M_U, R_U	Mathematical Identity

4.1.1 Detection of a "Pioneer-style" Anomaly In the DG framework, an observer on Earth is nested within a hierarchy of potential shadows (Earth, Sun, Milky Way, and Laniakea). As a probe moves radially outward from the Sun, the local field impedance Γ decreases as the Solar potential $\Phi_\odot(r) = GM_\odot/r$ attenuates. According to the unified identity:

$$dt_{probe} = dt_{earth}\sqrt{\frac{1 - \Phi_{ext}/c^2}{1 - (\Phi_{ext} + \Phi_\odot(r))/c^2}} \tag{52}$$

As $r \to \infty$, the probe clock exits the Solar shadow and begins to tick at the broader Laniakea-Machian rate. This manifest as a systematic blue-shift in the probe's internal frequency relative to a terrestrial baseline.

4.1.2 Proposed Deep-Space Test We propose a mission targeting a distance of $R \geq 200$ AU (the "Shadow Exit" zone). The probe must be equipped with an ultra-stable optical lattice clock with a frequency stability of 10^{-18} or better.

- **Detection Protocol**: Constant two-way frequency comparison between the probe and a terrestrial Hydrogen maser or optical clock baseline.
- **DG Prediction**: A non-linear frequency drift $\Delta\nu/\nu$ that correlates exactly with the dissipation of the $1/r$ Solar potential, eventually stabilizing at a constant "temporal surplus" as it enters the interstellar medium.
- **Standard Model Prediction (GR)**: A significantly smaller drift governed solely by the standard Schwarzschild metric, which lacks the Machian flux-impedance term.

4.1.3 Historical Context: Reinterpreting the Pioneer Anomaly The observed anomalous deceleration of the Pioneer 10 and 11 spacecraft[14, 15] ($a_p \approx 8.74 \times 10^{-10} m/s^2$) may be reinterpreted under this geometry. In DG, this is not a physical force, but a *chronometric artifact.*

Author contributions

Andrew Mueller is an independent researcher and the sole author.

References

[1] Tully R B and Fisher J R 1977 **54** 661–673

[2] Planck Collaboration et al 2020 *AA* **641** A1 URL https://doi.org/10.1051/0004-6361/201833880

[3] Planck Collaboration et al 2014 *AA* **571** A27 URL https://doi.org/10.1051/0004-6361/201321556

[4] Riess A G, Yuan W, Macri L M, Scolnic D, Brout D, Casertano S, Jones D O, Murakami Y, Anand G S, Breuval L, Brink T G, Filippenko A V, Hoffmann S, Jha S W, D'arcy Kenworthy W, Mackenty J, Stahl B E and Zheng W 2022 *The Astrophysical Journal Letters* **934** L7 ISSN 2041-8213 URL http://dx.doi.org/10.3847/2041-8213/ac5c5b

[5] Hafele J C and Keating R E 1972 *Science* **177** 166–170

[6] Einstein A *et al.* 1905 *Annalen der physik* **17** 891–921

[7] Gordon C, Land K and Slosar A 2008 *Monthly Notices of the Royal Astronomical Society* **387** 371–376 ISSN 0035-8711 URL https://doi.org/10.1111/j.1365-2966.2008.13239.x

[8] Singal A K 2022 *Monthly Notices of the Royal Astronomical Society* **511** 1819–1829 URL https://doi.org/10.1093%2Fmnras%2Fstac144

[9] Watkins R, Feldman H A and Hudson M J 2023 *The Astrophysical Journal* Finds local bulk flows in the 500 km/s range, supporting DG velocity values.

[10] Land-Strykowski M, Lewis G F and Murphy T 2025 *Monthly Notices of the Royal Astronomical Society* **543** 3229–3241 ISSN 0035-8711 (*Preprint* https://academic.oup.com/mnras/article-pdf/543/4/3229/64415852/staf1621.pdf) URL https://doi.org/10.1093/mnras/staf1621

[11] Rasouli A D, Tadayyoni H S, Baghram S and Rahvar S 2025 Addressing dipole tension via clustering in λcdm and beyond (*Preprint* 2508.18259) URL https://arxiv.org/abs/2508.18259

[12] Einstein, Albert 1916 *Annalen der Physik* **354** 769–822

[13] Dyson F W, Eddington A S and Davidson C 1920 A Determination of the Deflection of Light by the Sun's Gravitational Field, from Observations Made at the Total Eclipse of May 29, 1919 URL https://doi.org/10.1098/rsta.1920.0009

[14] Turyshev S G, Toth V T, Kinsella G, Lee S C, Lok S M and Ellis J 2012 *Phys. Rev. Lett.* **108**(24) 241101

[15] Anderson J D, Laing P A, Lau E L, Liu A S, Nieto M M and Turyshev S G 1998 *Phys. Rev. Lett.* **81**(13) 2858–2861